

# Study of gluon GPDs via vector meson production in ep and hh collisions

Ya-Ping Xie

Institute of Modern Physics, CAS  
Collaborated with S. V. Goloskokov and V. Goncalves  
Based on arXiv: 2408.05800, 2502.17743 and 2507.20448

Sep 23th, 2025

This slide focus on the gluon GPDs to study vector meson production. It contains follow sections:

- Introduction to GPDs
- Theoretical frame of vector meson production using GPDs method
- Differential cross section of  $J/\psi$  in GPDs method
- Production of  $J/\psi$  and  $\Upsilon$  at proton-proton collisions
- Production of  $J/\psi$  and  $\Upsilon$  at proton-lead UPCs
- Summary

Generalized Parton Distributions (GPDs) can be extracted from Deep Virtual Compton Scattering ( DVCS), Double Deep Virtual Compton Scattering(DDVCS) Time-like Compton Scattering (TCS) and Hard Exclusive Meson Production (HEMP) processes. GPDs can be employed to study

- Spin puzzle
- Energy Momentum tensor
- Gravitational form factor
- Mass radius, distributions and pressure

# Heavy vector meson production diagram

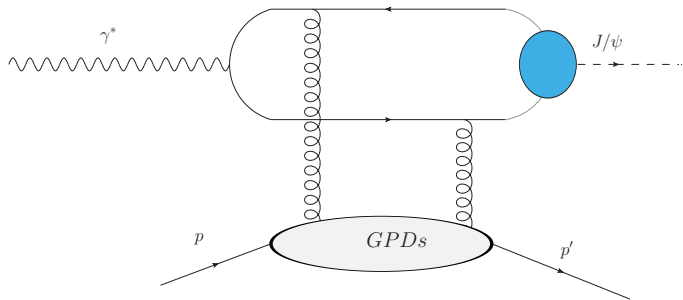


Figure 1: Typical diagram of heavy vector meson in photon-proton scattering.

GPDs can be employed to study meson production in several process.

- $\rho$  and  $\omega$  production ( gluon, up and down sea quark, and valence quark GPD)
- $\phi$  production (gluon and strange sea quark GPD)
- $J\psi$  and  $\Upsilon$  production (gluon GPD)
- Pseudoscalar mesons- polarized distributions

# Sum rules of GPDs

There are several kinds of GPD function,  $H_q, E_q, \tilde{H}_q, \tilde{E}_q$ . There are similar for gluon GPDs.

GPD connects parton distribution via  $H(x, 0, 0) = xf(x)$ . Hadron Form factor can be obtain from GPDs

$$\int dx H^q(x, \xi, t) = F_1^q(t), \quad \int dx E_q(x, \xi, t) = F_2^q(t); \quad (1)$$

$$\int dx \tilde{H}^q(x, \xi, t) = G_A^q(t), \quad \int dx \tilde{E}^q(x, \xi, t) = G_p^q(t). \quad (2)$$

Ji sum rules for the proton angular memonta

$$\int x dx (H^q(x, \xi, 0) + E^q(x, \xi, 0)) = 2J^q. \quad (3)$$

- GPDs  $H^q$  and  $E^q$  can be tested in  $\rho$  meson production
- $\tilde{H}^q$  and  $\tilde{E}^q$  can be tested in  $\pi^0$  production

Dipole model is employed to calculate vector mesons production in ep scattering. There are several models of the dipole amplitudes models, for example, IIM, IPsat, BGBK model. [PRD-74-074016 et al]

- Dipole model is valid in  $x_B < 0.01$  region
- It didn't consider the the skewness of the  $\xi$  effect
- It can not calculate the asymmetries of the vector mesons production

# Differential cross sections of vector mesons

The longitudinal and transversal differential cross sections as functions of  $|t|$  and total cross sections of heavy vector meson in photon-proton scattering as function of  $W$  and  $Q^2$  are calculated as

$$\frac{d\sigma_T}{dt} = \frac{1}{16\pi W^2(W^2 + Q^2)} [|\mathcal{M}_{++,++}|^2 + |\mathcal{M}_{+-,++}|^2], \quad (4)$$

$$\frac{d\sigma_L}{dt} = \frac{Q^2}{m_V^2} \frac{d\sigma_T}{dt}; \quad (5)$$

$$\frac{d\sigma}{dt} = \frac{d\sigma_T}{dt} + \varepsilon \frac{d\sigma_L}{dt}. \quad (6)$$

# Differential cross section of vector mesons

The gluon contribution to light vector meson electroproduction within GPD approach were calculated in [EPJC-42-281]. The helicity conservation amplitude of heavy vector meson production is given as

$$\begin{aligned} \mathcal{M}_{\mu'+,\mu+} &= \frac{e}{2} C_V \int_0^1 \frac{dx}{(x+\xi)(x-\xi+i\epsilon)} \\ &\times \{ \mathcal{H}_{\mu',\mu}^{V+} H_g(x, \xi, t, \mu_F) + \mathcal{H}_{\mu',\mu}^{V-} \tilde{H}_g(x, \xi, t, \mu_F) \}. \end{aligned} \quad (7)$$

While the helicity flip amplitude can be written as

$$\begin{aligned} \mathcal{M}_{\mu'-,\mu+} &= -\frac{e}{2} C_V \frac{\sqrt{-t}}{2m} \int_0^1 \frac{dx}{(x+\xi)(x-\xi+i\epsilon)} \\ &\times \{ \mathcal{H}_{\mu',\mu}^{V+} E_g(x, \xi, t, \mu_F) + \mathcal{H}_{\mu',\mu}^{V-} \tilde{E}_g(x, \xi, t, \mu_F) \}. \end{aligned} \quad (8)$$

Here the amplitudes  $\mathcal{H}_{\mu',\mu}^{V\pm}$  are determined as a sum and differences of amplitudes with different gluon helicities.

$$\mathcal{H}_{\mu',\mu}^{V\pm} = [\mathcal{H}_{\mu'+,\mu+}^V \pm \mathcal{H}_{\mu'-,\mu-}^V], \quad (9)$$

and flavor factor  $C_V = C_{J/\psi} = 2/3$ .

# Scattering amplitudes

There are 6 feynman diagrams of  $\gamma + p \rightarrow V + p$ . We must calculate the sum of feynman amplitudes of them

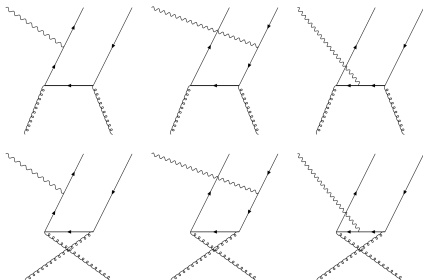


Figure 2: 6 Feynman diagrams of  $\gamma + g \rightarrow V + g$

# Scattering amplitudes

To calculate hard scattering amplitude we consider six gluon Feynman diagrams. After a length calculations, the hard amplitude can be cast into

$$\mathcal{H}_{\mu',\mu}^{V\pm}(x,\xi) = 64\pi^2 \alpha_s(\mu_R) \int_0^1 d\tau \int \frac{d^2\mathbf{k}_\perp}{16\pi^3} \psi(\tau, \mathbf{k}_\perp) \mathcal{F}_{\mu',\mu}^\pm(\tau, x, \xi, \mathbf{k}_\perp^2). \quad (10)$$

Here  $\tau$  and  $1 - \tau$  are the fraction of longitudinal part of quark (antiquark) momenta incoming to the meson wave function,  $\mathbf{k}_\perp$  is there transverse part. The  $k$ -dependent wave function of the vector meson is written as

$$\psi(\tau, \mathbf{k}_\perp) = a_v^2 f_v \exp\left(-a_v^2 \frac{\mathbf{k}_\perp^2}{\tau(1-\tau)}\right). \quad (11)$$

Here  $f_v$  is a  $J/\psi$  decay constant, the parameter  $a_v$  is fixed from the best fit  $J/\psi$  cross section and determine the average value of  $\langle \mathbf{k} \rangle_\perp^2$ .

# Hard part of scattering amplitude in $J/\psi$ production

For  $\tau = 1/2$ , the hard part of the amplitude can be written as

$$\mathcal{F}_{\mu',\mu}^{\pm} = \frac{f_{\mu',\mu}^{\pm}}{\text{denominator}} \quad (12)$$

$$\begin{aligned} \text{denominator} &= (2\mathbf{k}_{\perp}^2 + m_V^2 + Q^2)(4\xi\mathbf{k}_{\perp}^2 + (m_V^2 + Q^2)) \\ &(\xi - x) + i\epsilon)(4\xi\mathbf{k}_{\perp}^2 + (m_V^2 + Q^2)(\xi + x)) \end{aligned} \quad (13)$$

For longitudinal and transverse helicity conservation amplitudes  $f_{\mu,\mu}^{\pm}$  have a form

$$f_{00}^+ = -64\sqrt{Q^2}(m_V^2 + Q^2)^2(x^2 - \xi^2), \quad (14)$$

$$f_{11}^+ = 64m_V(m_V^2 + Q^2)^2(x^2 - \xi^2). \quad (15)$$

Here we omit  $k$  dependent terms. For the  $f_{\mu,\mu}^-$  which contains  $\tilde{H}$  contribution, we find that

$$f_{11}^- = -256(m_V^2 + Q^2)\mathbf{k}_{\perp}^2 m_V x \xi, \quad f_{00}^- = 0. \quad (16)$$

# GPDs function definitions

The GPDs are constructed adopting the double distribution representation

$$F(x, \xi, t) = \int_{-1}^1 d\beta \int_{-1+|\beta|}^{1-|\beta|} d\alpha \delta(\beta + \xi \alpha - x) f_g(\beta, \alpha, t), \quad (17)$$

$F$  with PDFs  $h$  via the double distribution functions  $f_i(\beta, \alpha, t)$ . For gluon double distribution functions, it is

$$f_g(\beta, \alpha, t) = e^{-b_V t} h_i(\beta, \mu_F) \frac{15 [(1 - |\beta|)^2 - \alpha^2]^2}{16 (1 - |\beta|)^5}. \quad (18)$$

The  $t$ -dependence in PDFs  $h(\beta, \mu_F)$  is the fitted from conlinear PDF (CT18NLO, NNPDF, ABMP)

# Ratio of the Re and Im of the amplitude

We can show the ratio of the Re and Im of the amplitudes.

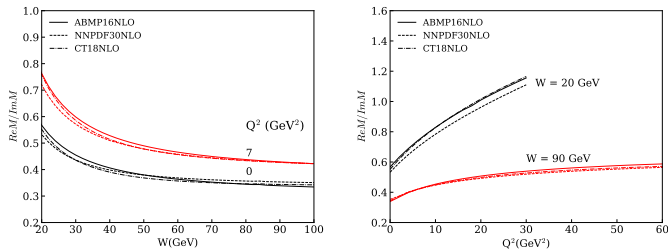
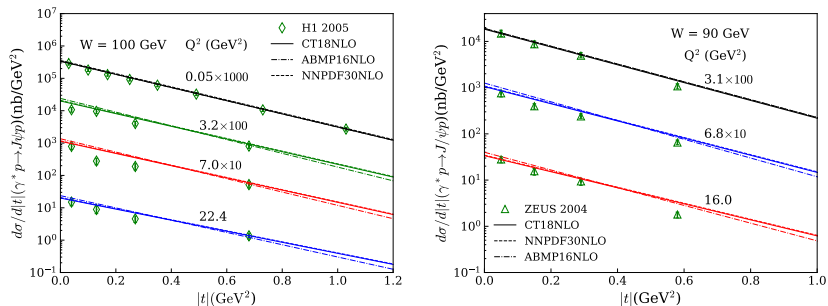


Figure 3: Ratio of  $ReM/ImM$  parts of  $J/\psi$  amplitudes at fixed  $W$  vs  $Q^2$ .

Ratio  $R = Re M / Im M$  of  $J/\psi$  amplitude at fixed  $Q^2$  and  $W$ .

- R-ratio at fixed  $Q^2$  decreases with  $W$  growing
- R-ratio at fixed  $W$  increases with  $Q^2$  growing
- At  $W \approx 20$  GeV (EicC), R-ratio is not far from unity
- At  $W \approx 90$  GeV (EIC), R-ratio is about 0.5

# $J/\psi$ production at different $|t|$



**Figure 4:**  $J/\psi$  differential cross section vs  $|t|$  at fixed  $W$  and different  $Q^2$ . The HERA experimental data are from from NPB-695-3 and EPJC-46-585. Cross sections are scaled by the factor shown in the graph.

- $t$ -dependencies of cross section at fix  $W$  and  $Q^2$  decrease well.
- The B-slope factor is good

# $J/\psi$ production at different $|t|$

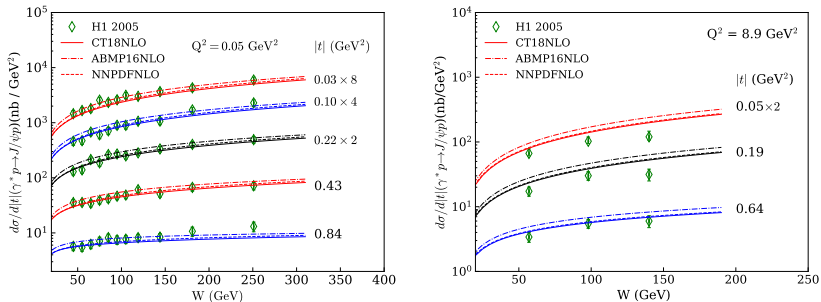


Figure 5:  $J/\psi$  differential cross section as a function of  $W$  at different  $|t|$ . The H1 experimental data are from EPJC-46-585.

- $t$ -dependencies of cross section at fix  $W$  and  $Q^2$  decrease well.
- The B-slope factor is good

# $J/\psi$ production at different $Q^2$

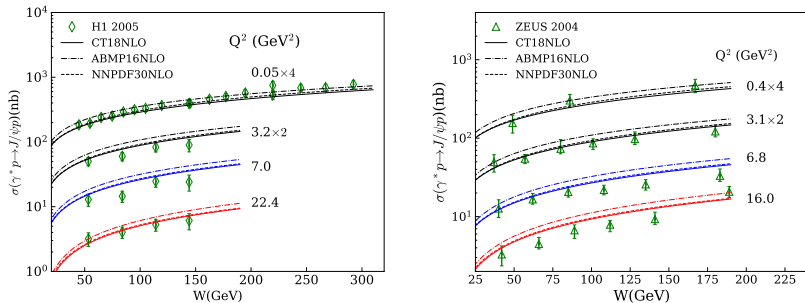


Figure 6:  $J/\psi$  total cross section vs  $W$  at different  $Q^2$  comparing with the HERA experimental data are taken from NPB-695-3 and EPJC-46-585.

- $Q^2$ -dependencies of cross section decrease well.
- $W$ -dependencies of total cross section is good.

# $J/\psi$ and $\Upsilon(1S)$ production in ep scattering

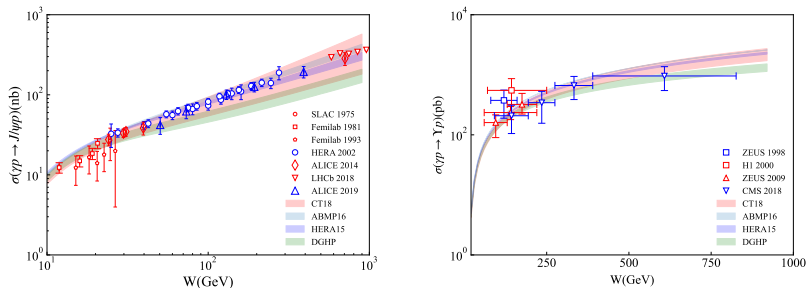


Figure 7:  $J/\psi$  and  $\Upsilon(1S)$  total cross section and at  $Q^2 = 0 \text{ GeV}^2$  vs  $W$  from low to very high energy.

- The model can describe the  $J/\psi$  photoproduction cross section at a large  $W$  region.
- Our calculation agree with the  $\Upsilon$  photoproduction cross sections.

# $J/\psi$ production at proton-proton ultraperipheral collisions

In proton-proton ultraperipheral collisions, the vector meson production can be obtained as [JHEP-1311-085]

$$\frac{d\sigma^{th}(pp)}{dy} = S^2(W_+) \left( k_+ \frac{dn}{dk_+} \right) \sigma_+^{th}(\gamma p) + S^2(W_-) \left( k_- \frac{dn}{dk_-} \right) \sigma_-^{th}(\gamma p). \quad (19)$$

$S(k)$  is the survival factors which have been studied in [JPG-44-03LT01]. The photon flux of the proton is given as

$$\frac{dn}{dk}(k) = \frac{\alpha_{em}}{2\pi k} \left[ 1 + \left( 1 - \frac{2k}{\sqrt{s}} \right)^2 \right] \left( \ln \Omega - \frac{11}{6} + \frac{3}{\Omega} - \frac{3}{2\Omega^2} + \frac{1}{3\Omega^3} \right). \quad (20)$$

# $J/\psi$ production at proton-proton ultraperipheral collisions

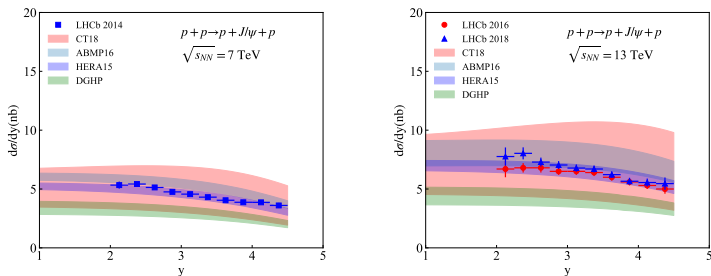


Figure 8:  $J/\psi$  production as a function of rapidity at pp UPC.

- The model can describe proton proton collision cross section at high energy.
- The cross section uncertainties of model is large since large uncertainties in gluon density. CT18NLO have a large uncertainties.

In proton-proton ultraperipheral collisions, the vector meson production can be obtained as

$$\frac{d\sigma^{th}(pPb)}{dy} = n(\omega)\sigma^{th}(\gamma p) \quad (21)$$

The photon flux of the lead is given as

$$n(\omega) = \frac{2Z^2\alpha_{em}}{\pi} \left[ \xi K_1(\xi)K_0(\xi) - \frac{\xi^2}{2} [K_1^2(\xi) - K_0^2(\xi)] \right], \quad (22)$$

where  $\xi = 2\omega R_A/\gamma_L$ , with  $R_A$  is the radius of the nucleus,  $K_0(x)$  and  $K_1(x)$  are the second kind of Bessel functions.

# $J/\psi$ production at p-Pb ultraperipheral collisions

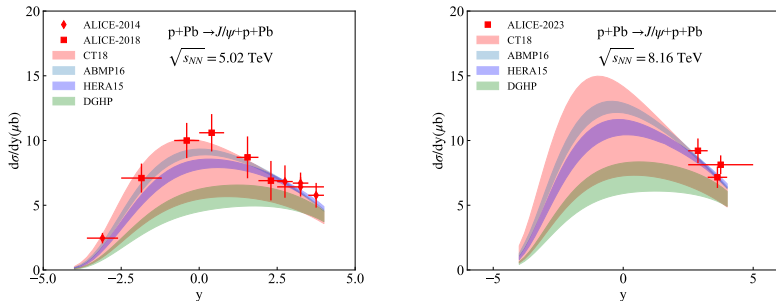


Figure 9:  $J/\psi$  production as a function of rapidity at p-Pb UPC.

- The model can describe  $J/\psi$  proton-lead collision cross section at high energy.
- The uncertainties is from the PDF uncertainties.

# $\Upsilon$ production at p-p and p-Pb ultraperipheral collisions

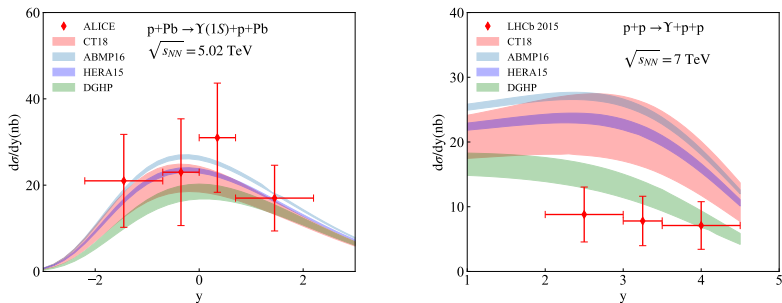


Figure 10:  $\Upsilon$  production as a function of rapidity at UPC.

We found that the model only can not describe the  $\Upsilon$  in p-p collisions.

We can conclude following conclusions:

- GPDs method can be employed to perform heavy vector mesons production in ep scattering and UPCs.
- Gluon density can be constrained via heavy vector meson cross sections in UPCs at high energy limit.
- Results of this work can be applied in future EicC experiments to give additional essential constraints on transversity GPDs at EicC energies range.
- Important information on gluon GPDs (especially  $E_g$ ,  $H_g$ ) can be obtained at US EIC, EicC and LHCb.

*Thanks for your attentions!*